Journal of Experimental Nanoscience
Publication details, including instructions for authors and subscription information:
http://www.informaworld.com/smpp/title~content=t716100757

Zirconia nanoparticles: a martensitic phase transition at low temperature

S. Jiménez[a]; S. Carmona[bc]; Victor M. Castaño[c]
[a] Universidad Tecnológica de San Juan del Río, San Juan del Río, Querétaro, México [b] Facultad de Estudios Superiores Cuautitlán, Universidad Nacional Autónoma de México, Atlanta, México [c] Centro de Física Aplicada y Tecnología Avanzada, Universidad Nacional Autónoma de México, Querétaro, México

To cite this Article Jiménez, S. , Carmona, S. and M. Castaño, Victor(2009) 'Zirconia nanoparticles: a martensitic phase transition at low temperature', Journal of Experimental Nanoscience, 4: 1, 95 — 103
To link to this Article: DOI: 10.1080/17458080802570633
URL: http://dx.doi.org/10.1080/17458080802570633

Journal of Experimental Nanoscience
Vol. 4, No. 1, March 2009, 95–103

Taylor & Francis
Taylor & Francis Group

Zirconia nanoparticles: a martensitic phase transition at low temperature

S. Jiménez[a], S. Carmona[bc] and Victor M. Castaño[c]*

[a]*Universidad Tecnológica de San Juan del Río, San Juan del Río, Querétaro, México;* [b]*Facultad de Estudios Superiores Cuautitlán, Universidad Nacional Autónoma de México, Atlanta, México;* [c]*Centro de Física Aplicada y Tecnología Avanzada, Universidad Nacional Autónoma de México, Querétaro, México*

(*Received 5 September 2008; final version received 20 October 2008*)

The low temperature (450–600°C) amorphous to tetragonal and tetragonal to monoclinic phase transformations in zirconia nanoparticles, produced by an aqueous sol–gel route, are analysed in terms of their changes of lattice parameters and by using the phenomenological theory of martensitic transformation (Bowles–Mackenzie theory) to explore whether or not those crystallographic changes may be considered a martensitic transformation within the zirconia nanoparticles.

Keywords: zirconia nanoparticles; martensitic transformation; tetragonal phase; monoclinic phase; Bowles–Mackenzie theory

1. Introduction

Zirconia and its compounds have represented a very attractive family of materials for a wide range of high-tech applications since the first modern reports on their properties [1–5]. More specifically, the polymorphic nature of pure zirconia has received extensive attention due both to the scientific phenomena behind the transformations involved and to its potential engineering uses [4,5]. Pure zirconia exhibits three well-defined crystallographic forms, namely the monoclinic, tetragonal, and cubic polymorphs. The tetragonal phase, normally stable at high temperature for the case of coarse grain ceramics, has been observed stable or metastable at room temperature [6]. Since Ruff and Ebert's [1] pioneering report in 1929 on the existence of a reversible tetragonal to monoclinic martensitic transformation in pure zirconia, much effort has been dedicated to understanding the details of this transformation. Today, for example, it is well known that, at about 1170°C, a martensitic transformation from tetragonal to monoclinic symmetry takes place in ambient condition [2,7]. In 1963, Wolten was the first to suggest that this tetragonal–monoclinic transformation was martensitic in nature. He based his suggestion on the similarity of the two crystallographic forms [8].

Calculations of the martensitic transformations have been carried out by Bansal and Heuer [9], using the Bowles–McKenzie phenomenological theory [10], and

*Corresponding author. Email: castano@fata.unam.mx

ISSN 1745–8080 print/ISSN 1745–8099 online

DOI: 10.1080/17458080802570633
http://www.informaworld.com

Kriven et al. [11] developed calculations of a possible crystallographic transformation mechanism on bulk, unconstrained zirconia crystals.

As for the effect of grain size, it has been observed that zirconia particles with different sizes modify the phase fields of tetragonal, tetragonal + monoclinic, and monoclinic variants, with increased grain size, respectively [12,13]. In any case, the effect of nanometre-sized grains and/or particles, seems to lead to interesting properties in ceramics materials [14].

In this article, a series of calculus based on the Bowles–Mckenzie theory, by using the lattice parameters experimentally obtained from zirconia nanoparticles synthesised *ad hoc*, is presented, to explore whether or not the crystallographic changes reported by a number of authors in zirconia nanoparticles [14–18] may be considered a martensitic transformation, as opposed to what is accepted in bulk zirconia.

2. Experimental

Zirconium carbonate paste was utilised in order to prepare a stock solution 1 M in Zr from distilled, deionised water for all the experimental work, according to the following reaction scheme [15]:

$$2[Zr_2(CO_3)(OH)_2O_2] + 2NH_4OH + H_2O \rightarrow (NH_4)_2[Zr(CO_3)_2(OH)_2] + 3Zr(OH)_4 + nH_2O$$

Portions of the 1 M zirconyl stock solution were adjusted to pH values between 12 and 13, by adding ammonia. A small amount of precipitate was redissolved upon heating. The clear solutions were then refluxed and samples removed at various time intervals. The samples were cooled down to room temperature and their pH recorded as a function of viscocity until total solidification, after which, the resulting transparent specimens were powdered and subjected to a heat treatment at up to 610°C. XRD patterns were recorded at regular intervals between 200°C and 610°C in a Siemens D-5000 machine. A JEOL 100-CX apparatus, operating a 100 keV was utilised for obtaining micrographs of the grinded samples, deposited onto C-coated Cu microscope grids.

3. Results and discussion

The relationship between viscosity and pH during the solidification process is summarised in the plot of Figure 1, for three typical samples, to show the reproducibility of the process. All the samples solidified between 300 and 500 cps and at pH = 9.58, approximately. The highly transparent monoliths obtained (see Figure 2), consisted of 8 nm particles, on the average, as can be appreciated in the TEM micrograph (Figure 3).

The series of X-ray diffractograms (Figure 4) show that, initially, a transformation from amorphous to tetragonal structure occurs at 400°C, approximately. Then, between 400°C and 550°C the tetragonal phase develops continuously. At 600°C, the monoclinic and tetragonal phases coexist.

By using Ito's [19] method to analyse the diffraction data, summarised in Figure 4, for tetragonal zirconia, the lattice parameters are: $a = b = 0.4999992$ nm, $c = 0.5092005$ nm, whereas for monoclinic zirconia, the Ito's method shows that the lattice parameters were: $a = 0.5110305$ nm, $b = 0.5231009$ nm, $c = 0.5270408$ nm, and $\beta = 96.884570$.

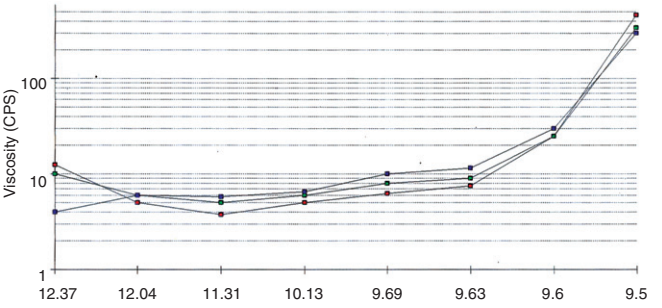

Figure 1. Viscosity *vs*. pH during the solidification of the samples.

Figure 2. Photograph of the monoliths obtained.

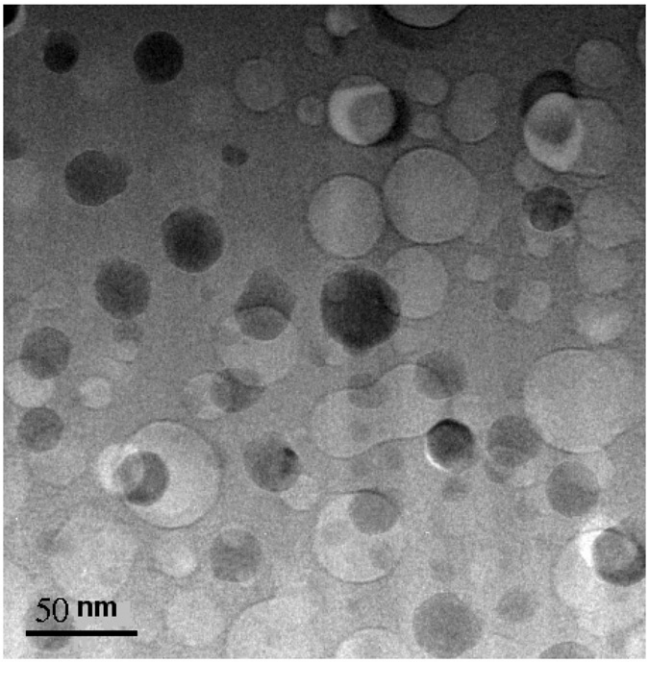

Figure 3. TEM micrograph of the monoliths.

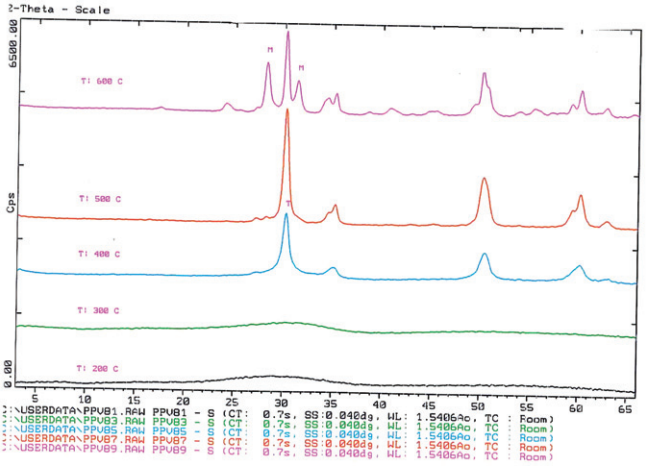

Figure 4. X-ray diffractograms of samples after heat treatments at the temperatures shown.

Thus, a low temperature phase transformation can be described by a series of matrices, according to Niggli's [20] method.

Now, according to Bowles and McKenzie, for a martenstic transformation, the principal axes are determined by the nonzero solutions of the equations:

$$\{(\mathrm{AC'B})(\mathrm{B^*GB})(\mathrm{BCA}) - \eta_i^2(\mathrm{A^*GA})\}[\mathrm{A;\ X}] = 0 \tag{1}$$

where (BCA) is the Bain [21] correspondence matrix between the initial phase (A) and the final phase B, (AC′B) is the transpose of (BCA), (B*GB) and (A*GA) are the metrics for the final and initial phases, respectively, A* and B* are the reciprocal lattices for the initial and final phases, respectively.

Then, for the tetragonal to monoclinic phase transformation in zirconia, by using our experimental data, Equation (1) becomes:

$$\{(\mathrm{TC'M})(\mathrm{M^*GM})(\mathrm{MCT}) - \eta_i^2(\mathrm{T^*GT}\}[\mathrm{T;\ X}] = 0 \tag{2}$$

where T is the tetragonal lattice and M is the monoclinic lattice.

The magnitudes and directions of the principal strains of the Bain deformation, η_{i}, are the eigenvalues and eigenvectors of Equation (2) in the procedure developed by Bowles and McKenzie. Moreover, there are three types of lattice correspondences between the tetragonal and monoclinic phases in pure zirconia [11], i.e.,

$$(\mathbf{MCT})a = \begin{pmatrix} 0 & 1 & 0 \\ 0 & 0 & 1 \\ 1 & 0 & 0 \end{pmatrix} \tag{3}$$

$$(\mathbf{MCT})b = \begin{pmatrix} \mathbf{1} & \mathbf{0} & \mathbf{0} \\ \mathbf{0} & \mathbf{0} & \mathbf{-1} \\ \mathbf{0} & \mathbf{1} & \mathbf{0} \end{pmatrix} \tag{4}$$

$$(\mathbf{MCT})c = \begin{pmatrix} \mathbf{1} & \mathbf{0} & \mathbf{0} \\ \mathbf{0} & \mathbf{1} & \mathbf{0} \\ \mathbf{0} & \mathbf{0} & \mathbf{1} \end{pmatrix} \tag{5}$$

Further, the two metrics for tetragonal and monoclinic phases are

$$(\mathrm{T}^{*}\mathrm{GT}) = \begin{pmatrix} a_{\mathrm{t}} & 0 & 0 \\ 0 & b_{\mathrm{t}} & 0 \\ 0 & 0 & c_{\mathrm{t}} \end{pmatrix} \tag{6}$$

$$(\mathrm{M}^{*}\mathrm{GM}) = \begin{pmatrix} a_{\mathrm{m}} & 0 & a_{\mathrm{m}}c_{\mathrm{m}}\cos\beta_{\mathrm{m}} \\ 0 & b_{\mathrm{m}} & 0 \\ a_{\mathrm{m}}c_{\mathrm{m}}\cos\beta_{\mathrm{m}} & 0 & c_{\mathrm{m}} \end{pmatrix} \tag{7}$$

where a_{t}, b_{t}, c_{t}, and b_{m}, c_{m} are the experimentally obtained lattice parameters for the tetragonal and monoclinic phases, respectively, and β_{m} is the monoclinic angle. Nevertheless, the lattice correspondences have different variants according to Bansal and Heuer [9]. Table 1 shows all the possible variants for the lattice correspondences A, B, and C, whereas Table 2 shows equations defining the principal deformations after applying Equation (2). Table 3 shows the eigenvalues obtained after solving the equations in Tables 2, and Table 4 shows the eigenvectors related to the eigenvalues obtained via Equation (2) and shown in Table 2. Finally, Table 5 shows the normalised eigenvectors, which occur in Table 4. It is worth noticing from Table 4 the fact that $\mathrm{A}_4 \equiv \mathrm{A}_2$, $\mathrm{A}_3 \equiv \mathrm{A}_1$, $\mathrm{B}_1 \equiv \mathrm{A}_2$, $\mathrm{B}_2 \equiv \mathrm{A}_3 \equiv \mathrm{A}_1$, $\mathrm{B}_3 \equiv \mathrm{A}_2$, $\mathrm{B}_4 \equiv \mathrm{B}_2$, and $\mathrm{C}_1 \equiv \mathrm{C}_2 \equiv \mathrm{C}_3 \equiv \mathrm{C}_4$ and eigenvectors in Table 4 is reduced to seven normalised eigenvectors only. We find three real eigenvectors, which form an orthogonal set. The deformation matrix representing the Bain strain, which converts the tetragonal zirconia lattice to the monoclinic zirconia lattice is given by:

$$(\mathrm{MA_1T}) = \begin{pmatrix} \eta_1 & 0 & 0 \\ 0 & \eta_2 & 0 \\ 0 & 0 & \eta_3 \end{pmatrix} = \begin{pmatrix} 0.979111 & 0 & 0 \\ 0 & 1.027390 & 0 \\ 0 & 0 & 1.094098 \end{pmatrix}$$

Now, if a new orthonormal basis is defined, consisting of unit basis parallel vectors $[\mathrm{A}_1, \mathrm{v}_1] = [-0.600465, 0.799651, 0.000005]$, $[\mathrm{A}_1, \mathrm{v}_2] = [-0.799646, -0.600472, -0.000002]$, and $[\mathrm{A}_1, \mathrm{v}_3] = [0.000033, 0.000015, 0.999999]$.

After the magnitudes and directions of the principal axes on the lattice deformation have been obtained from the Equation (2), the locus of initial directions of all vectors, which are not changed in length by the lattice deformation, known as the initial Bain cone, can be obtained, as well [21].

Therefore, the Bowles–Mackenzie analysis of our experimental data, which on the other hand, agrees with previous reports [22–24], indicated that the transformation can be indeed regarded as a martensitic one.

Phenomenologically speaking, Hunter et al. [25] found that, for tetragonal zirconia, the shift in oxygen δ was simply related to the lattice parameters via the relation $\delta = 0.24(1 - a^2/c^2)^{1/2}$, independently of the dopant. This is highly relevant to the present work because the oxygen position and bond lengths can be determined by merely

Table 1. Different lattice correspondence matrices for zirconia.

Lattice correspondence matrices	1	2	3	4
A	$\begin{pmatrix}0&1&0\\0&0&1\\1&0&0\end{pmatrix}$	$\begin{pmatrix}0&0&-1\\0&1&0\\1&0&0\end{pmatrix}$	$\begin{pmatrix}0&-1&0\\0&0&-1\\1&0&0\end{pmatrix}$	$\begin{pmatrix}0&0&1\\0&-1&0\\1&0&0\end{pmatrix}$
B	$\begin{pmatrix}0&0&1\\1&0&0\\0&1&0\end{pmatrix}$	$\begin{pmatrix}-1&0&0\\0&0&1\\0&1&0\end{pmatrix}$	$\begin{pmatrix}0&0&-1\\-1&0&0\\0&1&0\end{pmatrix}$	$\begin{pmatrix}1&0&0\\0&0&-1\\0&1&0\end{pmatrix}$
C	$\begin{pmatrix}1&0&0\\0&1&0\\0&0&1\end{pmatrix}$	$\begin{pmatrix}0&-1&0\\1&0&0\\0&0&1\end{pmatrix}$	$\begin{pmatrix}-1&0&0\\0&-1&0\\0&0&1\end{pmatrix}$	$\begin{pmatrix}0&1&0\\-1&0&0\\0&0&1\end{pmatrix}$

Table 2. Equation defining the principal strains.

LC	Equation defining the principal strains
A_1	$-16205.1829\eta_i^6 + 52038.7005\eta_i^4 - 55469.9685\eta_i^2 + 19629.1201 = 0$
A_2	$-16205.1829\eta_i^6 + 52067.7940\eta_i^4 - 55509.8984\eta_i^2 + 19629.1205 = 0$
A_3	$-16205.1829\eta_i^6 + 52038.7005\eta_i^4 - 55469.9684\eta_i^2 + 19629.1201 = 0$
A_4	$-16205.1829\eta_i^6 + 52067.7940\eta_i^4 - 55509.8984\eta_i^2 + 19629.1205 = 0$
B_1	$-16205.1829\eta_i^6 + 52067.7940\eta_i^4 - 555609.8984\eta_i^2 + 19629.1205 = 0$
B_2	$-16205.1824\eta_i^6 + 52038.7005\eta_i^4 - 55469.9683\eta_i^2 + 19629.1201 = 0$
B_3	$-16205.1829\eta_i^6 + 52067.7940\eta_i^4 - 55509.8984\eta_i^2 + 19629.1205 = 0$
B_4	$-16205.1829\eta_i^6 + 52038.7005\eta_i^4 - 55469.9685\eta_i^2 + 19629.1201 = 0$
C_{1*}	$-16205.1829\eta_i^6 + 52029.2117\eta_i^4 - 55467.6836\eta_i^2 + 19629.1199 = 0$

Note: LC = lattice correspondence, $*C_1 = C_2 = C_3 = C_4$.

measuring the ratio of the lattice parameters, as obtained experimentally from X-ray diffraction data. They assert that the coefficient in the expression would be 0.25 if one assumed the atoms to be hard spheres, and hence the slight difference could be thought of as a slight softening.

4. Conclusions

The atomic displacements involved in the transformation from tetragonal to monoclinic zirconia nanoparticles were described in terms of the corresponding

Table 3. Eigenvalues (derived from equations in Table 2 and Equation (2)).

LC	η_1^2	η_2^2	η_3^2	η_1	η_2	η_3
A_1	0.958659	1.055530	1.197050	0.979111	1.027390	1.094098
A_2	0.935327	1.094740	1.182970	0.967123	1.046298	1.087644
A_3	0.958660	1.055530	1.197050	0.979112	1.027390	1.094098
A_4	0.935327	1.094740	1.182970	0.967123	1.046298	1.087644
B_1	0.935327	1.094740	1.182970	0.967123	1.046298	1.087644
B_2	0.958660	1.055530	1.197050	0.979112	1.027390	1.094098
B_3	0.935327	1.094740	1.182970	0.967123	1.046298	1.087644
B_4	0.958660	1.055530	1.197050	0.979111	1.027390	1.094098
C_1	0.944731	1.094880	1.171040	0.971973	1.046365	1.082146

Note: LC = lattice correspondence.

Table 4. Eigenvectors (which emerge from eigenvalues in Table 3 via Equation (2)).

Eigenvalue + Lattice correspondence	Eigenvector related (not normalised)
$\eta_1^2 + A_1$	[−38754.1, 51609.6, 0.381660]
$\eta_2^2 + A_1$	[0.386163, 0.181412, 11599.2]
$\eta_3^2 + A_1$	[−11970.6, −8988.99, −0.326233]
$\eta_1^2 + A_2$	[−0.031736, 0.375581, −0.300095]
$\eta_2^2 + A_2$	[0.517704, 0.308602, −1.000010]
$\eta_3^2 + A_2$	[3.789110, 2.792750, −0.349092]
$\eta_1^2 + A_3$	[−38754.1, 51609.6, 0.381660]
$\eta_2^2 + A_3$	[0.386163, 0.181412, 11599.2]
$\eta_3^2 + A_3$	[−11970.6, −8988.99, −0.326233]
$\eta_1^2 + A_4$	[−0.031736, 0.375581, −0.300095]
$\eta_2^2 + A_4$	[0.517704, 0.308602, −1.000010]
$\eta_3^2 + A_4$	[3.789110, 2.792750, −0.349092]
$\eta_1^2 + B_1$	[−0.031736, 0.375581, −0.300095]
$\eta_2^2 + B_1$	[0.517704, 0.308602, −1.000010]
$\eta_3^2 + B_1$	[3.789110, 2.792750, −0.349092]
$\eta_1^2 + B_2$	[−38754.1, 51609.6, 0.381660]
$\eta_2^2 + B_2$	[0.386163, 0.181412, 11599]
$\eta_3^2 + B_2$	[−11970.6, −8988.99, −0.326233]
$\eta_1^2 + B_3$	[−0.031736, 0.375581, −0.300095]
$\eta_2^2 + B_3$	[0.517704, 0.308602, −1.000010]
$\eta_3^2 + B_3$	[3.789110, 2.792750, −0.349092]
$\eta_1^2 + B_4$	[−38754.1, 51609.6, 0.381660]
$\eta_2^2 + B_4$	[0.386163, 0.181412, 11599.2]
$\eta_3^2 + B_4$	[−11970.6, −8988.99, −0.326233]
$\eta_1^2 + C_1$ (or C_2 or C_3 or C_4)	[−0.156817, 0.558056, 0.328837]
$\eta_2^2 + C_1$ (or C_2 or C_3 or C_4)	[0.518393, 0.309187, −1.073200]
$\eta_3^2 + C_1$ (or C_2 or C_3 or C_4)	[2.043030, 1.479210, −0.391010]

Table 5. Normalised eigenvectors (along the principal axes) for the principal strains (calculated using Equation (2)).

Eigenvalue + Lattice correspondence	Eigenvector related (normalised)
$\eta_1 + A_1$	$[A_1, v_1] = [-0.600465, 0.799651, 0.000005]$
$\eta_2 + A_1$	$[A_1, v_2] = [0.000033, 0.000015, 0.999999]$
$\eta_3 + A_1$	$[A_1, v_3] = [-0.799646, -0.600472, -0.000002]$
$\eta_1 + A_2$	$[A_2, v_1] = [-0.065863, 0.779547, 0.622870]$
$\eta_2 + A_2$	$[A_2, v_2] = [0.443398, 0.264306, -0.856470]$
$\eta_3 + A_2$	$[A_2, v_3] = [0.802773, 0.591681, -0.073959]$
$\eta_1 + C_1$	$[C_1, v_1] = [-0.235303, 0.837360, 0.493418]$
$\eta_2 + C_3$	$[C_1, v_2] = [0.421012, 0.251105, -0.871605]$
$\eta_3 + C_2$	$[C_1, v_3] = [0.800424, 0.579529, -0.153191]$

changes of lattice parameters. According to the findings by various groups, the monoclinic phase in zirconia would arise as a necessary consequence of the fact that Zr and O atomic displacements constitute a common homogeneous deformation, followed by heterogeneous atomic displacements. On the other hand, and based on the Bowles–Mackenzie theory, our mathematical analysis has shown that the tetragonal to monoclinic transformation can indeed be regarded as a low-temperature martensitic transformation, occuring thanks to the high stress concentrations, in turn due to the small particle size.

References

[1] O. Ruff and F.Z. Ebert, *Ceramics of highly refractory materials*, Anorg. Allgem. Chem. 180 (1929), pp. 19–41.
[2] Y.L. Zhang, X.J. Jin, Y.H. Rong, T.Y. Hsu, D.Y. Jiang, and J.L. Shi, *The size dependence of structural stability in nano-sized ZrO_2 particles*, Mater. Sci. Eng. A 438–440 (2006), pp. 399–402.
[3] B. Basu, *Toughening of yttria-stabilised tetragonal zirconia ceramics*, Int. Mater. Rev. 50 (2005), pp. 239–256.
[4] F.A. Mumpton and R. Roy, *Low-temperature equilibria among ZrO_2, ThO_2, and UO_2*, J. Am. Ceram. Soc. 43 (1960), pp. 234–240.
[5] R.H.J. Hannink, P.M. Kelly, and B.C. Muddle, *Transformation toughening in Zirconia-containing ceramic*, J. Am. Ceram. Soc. 83 (2000), pp. 461–487.
[6] S. Shukla and S. Seal, *Mechanisms of room temperature metastable tetragonal phase stabilisation in zirconia*, Int. Mater. Rev. 50 (2005), pp. 45–64.
[7] B. Basu, J. Vleugels, and O. Van der Biest, *Toughness tailoring of yttria-doped zirconia ceramics*, Mater. Sci. and Eng. A 380 (2004), pp. 215–221.
[8] G.M. Wolten, *Diffusionless phase transformations in Zirconia and Hafnia*, J. Am. Ceram. Soc. 46 (1963), pp. 418–422.
[9] G.K. Bansal and A.H. Heuer, *On a martensitic phase transformation in zirconia (ZrO2)–II. Crystallographic aspects*, Acta Metall. 22 (1974), pp. 409–417.
[10] J.S. Bowles and J.K. Mackenzie, *The crystallography of martensite transformations I*, Acta Metall. 2 (1954), pp. 129–138.
[11] W.M. Kriven, C.M. Wayman, D.A. Payne, H. Chen J.D. Bass, *Displacive transformations in ceramics*, Air Force Office of Scientific Research.
[12] B. Wang, *Some special characteristics of stress-induced martensitic transformations predicted by a statistical model*, Acta Mater. 45 (1996), pp. 1551–1556.

[13] I.W. Chen, Y.H. Chiao, and K. Tsuzaki, *Theory and experiment of martensitic nucleation in ZrO_2 containing ceramics and ferrous alloys*, Acta Metall. 33 (1985), pp. 1847–1859.
[14] D. Mendoza, C. Angeles, P. Salas, R. Rodríguez, and V.M. Castaño, *Nanoparticles-enhanced thermoluminescence in silica gels*, Nanotechology 14 (2003), pp. L19–L22.
[15] S. Jiménez, A. Valadéz, E. Rubio, and V.M. Castaño, *Infiltration of glassy bodies with zirconia nanoparticles*, J. Nanopart. Res. 5 (2003), pp. 173–177.
[16] P. Salas, E. De la Rosa, D. Mendoza, P. González, R. Rodríguez, and V.M. Castaño, *High temperature thermoluminescence induced on UV-irradiated tetragonal zirconia prepared by sol-gel*, Mater. Lett. 45 (2000), pp. 241–248.
[17] J.Ch. Valmalette and M. Isa, *Size effects on the stabilization of ultrafine Zirconia nanoparticles*, Chem. Mater. 14 (2002), pp. 5098–5102.
[18] D. Vollath and K.E. Sickafus, *Synthesis of nanosized ceramic oxide powders by microwave plasma reactions*, Nanostruct. Mater. 1 (1992), pp. 427–431.
[19] I.G. Kamaeva and V.V. Serebrennikov, *A program for indexing x-ray diffraction patterns of polycrystalline substances with low symmetry*, J. Struct. Chem. 9 (1968), pp. 625–626.
[20] A. Niggli, V.V. Vand, and R. Pepinsky, *The optimal shift method for refinement of crystal structures*, Acta Cryst. 13 (1960), pp. 1002–1010.
[21] Y.L. Zhang, X.J. Jin, Y.H. Rong, T.Y. Hsu, D.Y. Jiang, and J.L. Shi, *On the t→ m martensitic transformation in Ce-Y-TZP ceramics*, Acta Mater. 54 (2006), pp. 1289–1295.
[22] P. Salas, J. Montoya, V.M. Castaño, and R. Rodríguez, *Segregation effects in sol-gef zirconia-silica materials analyzed through their radial distribution functions*, Mater. Res. Innov. 3 (2000), pp. 205–215.
[23] S. Jiménez, C. López, R. Fuertes, and V.M. Castaño, *Synthesis of an $AlZrO_2$ composite by infiltration of Zr-chelates into an Al matrix*, J. Nanopart. Res. 5 (2003), pp. 173–179.
[24] V.G. Zavodinsky and A.N. Chibisov, *Zirconia nanoparticles and nanostructured systems*, J. Phys.: Conf. Ser. 29 (2006), pp. 173–176.
[25] B.A. Hunter, C.J. Howard, and D.J. Kim, *Neutron diffraction study of tetragonal zirconias containing Sn*, Physica B: Condens. Mat. 241–243 (1999), pp. 1249–1251.